

"In presenting the dissertation as a partial fulfillment of the requirements for an advanced degree from the Georgia Institute of Technology, I agree that the Library of the Institution shall make it available for inspection and circulation in accordance with its regulations governing materials of this type. I agree that permission to copy from, or to publish from, this dissertation may be granted by the professor under whose direction it was written, or such copying or publication is solely for scholarly purposes and does not involve potential financial gain. It is understood that any copying from, or publication of, this dissertation which involves potential financial gain will not be allowed without written permission.

---

12T

A STUDY OF ECCENTRICALLY CURVED  
BEAMS OF LOW SECTION RATIO


A THESIS

Presented to  
the Faculty of the Graduate Division  
Georgia Institute of Technology

In Partial Fulfillment  
of the Requirements for the Degree  
Master of Science

By  
Joseph Crump Durden, Jr.

June 1954



A STUDY OF ECCENTRICALLY CURVED  
BEAMS OF LOW SECTION RATIO

Approved:

\_\_\_\_\_  
\_\_\_\_\_  
\_\_\_\_\_  
\_\_\_\_\_  
\_\_\_\_\_

Date Approved by Chairman: June 1, 1954

## PREFACE

The basic problem considered in this project is not the original idea of the author of this thesis. Instead, this investigation was performed to expand the known information about eccentrically curved beams into regions not previously studied. The photoelastic method was used to investigate beams having a section ratio below ten.

The real challenge appeared in the design of equipment and the development of techniques required for the production of accurate models of the sizes and shapes needed. The simple jig for cutting circular arcs, for example, was the result of many attempts to cut smooth, accurate arcs on a plastic model.

As the project progressed many interesting facts were brought to light. Perhaps the most interesting feature was the relative consistency of results obtained from photoelastic determinations. Due to the many variables involved, it is quite possible for errors to arise from many sources. Some deviations did occur, but most of these can be attributed to experimental factors.

The writer takes this opportunity to express his gratitude to his thesis advisor, Dr. Joseph P. Vidosic, Professor of Mechanical Engineering at the Georgia Institute of Technology. Dr. Vidosic not only suggested this project, but he gave much valuable time and assistance in its execution. Also, appreciation is extended to the other members of the thesis committee, Dr. Homer S. Weber and Professor Francis M. Hill. Their useful suggestions and constructive comments aided materially in the writing of this thesis.

## TABLE OF CONTENTS

	Page
PREFACE. . . . .	ii
LIST OF TABLES . . . . .	iv
LIST OF ILLUSTRATIONS. . . . .	v
ABSTRACT . . . . .	vi
CHAPTER	
I. INTRODUCTION. . . . .	1
II. INSTRUMENTATION AND EQUIPMENT . . . . .	4
Material	
Equipment	
Cutting	
The Polariscope	
Photographic Equipment	
III. PROCEDURE . . . . .	8
IV. DISCUSSION OF RESULTS . . . . .	12
Arch Beams	
Crescent I Beams	
Crescent II Beams	
V. CONCLUSIONS . . . . .	25
VI. RECOMMENDATIONS . . . . .	27
APPENDIX . . . . .	29
NOMENCLATURE . . . . .	41
BIBLIOGRAPHY . . . . .	42

## LIST OF TABLES

Table	Page
1. Calibration Data - CR 39. . . . .	30
2. Arch Beam Data. . . . .	31
3. Crescent I Data . . . . .	32
4. Crescent II Data. . . . .	33
5. Location of Neutral Surface at Central Section. . . . .	37
6. Stresses in Non-Central Sections for Arch Beams at Inside Boundary. . . . .	38
7. Stresses in Non-Central Sections at Inside Boundary for Crescent I Beams. . . . .	39
8. Stresses in Non-Central Sections at Inside Boundary for Crescent II Beams . . . . .	40

## LIST OF ILLUSTRATIONS

Figure	Page
1. Types of Curved Beams. . . . .	3
2. Jig for Cutting Arcs . . . . .	6
3. Loading Frame with Model . . . . .	6
4. Full Size Drawings of Typical Models . . . . .	9
5. Stress Factors for Arch Beams. . . . .	14
6. Photograph and Stress Distribution Curve for an Arch Beam . . . . .	15
7. Location of Neutral Axis . . . . .	16
8. Stress Factors for Crescent I Beams. . . . .	19
9. Photograph and Stress Distribution Curve for a Crescent I Beam. . . . .	20
10. Stress Factors for Crescent II Beams . . . . .	22
11. Photograph and Stress Distribution Curve for a Crescent II Beam . . . . .	23
12. Photograph and Stress Distribution Curve for Crescent I No. 1 . . . . .	28
13. Plot of Stress Factors and Reciprocals of Section Ratios for Arch Beams. . . . .	34
14. Plot of Stress Factors and Reciprocals of Section Ratios for Crescent I Beams. . . . .	35
15. Plot of Stress Factors and Reciprocals of Section Ratios for Crescent II Beams . . . . .	36

A STUDY OF ECCENTRICALLY CURVED BEAMS  
OF LOW SECTION RATIO

Joseph C. Durden, Jr.

ABSTRACT

Stresses in three types of eccentrically curved beams have been investigated photoelastically for beams having low section ratios. Stress factors have been expressed in empirical formulae for the range considered. These beams have circular arc boundaries with different centers. The cross-section is rectangular, and the section depth varies along the span of the beam. The models used in this study were symmetrical with respect to the central section and were loaded in pure bending.

Stress factors were obtained as the ratio of observed stress to computed stress in corresponding straight beams. The parameter for comparing stress factors is the section ratio, the ratio of the sum of the outer and inner radii to the depth of the central section. The section ratios studied extended from ten to as low a value as practical.

The classification of the three types of eccentrically curved beams depends upon the geometrical shapes. The "Arch" beam is the type in which the depth of section is smallest at the central section and increases with the distance from the central section. The "Crescent" is the type which has a corresponding decrease in section. There are two divisions of the Crescent type. Crescent I has an outer radius larger than the inner radius, while Crescent II has an outer radius smaller than the inner radius.

Empirical equations were established to express the variation of stress factors with section ratios for the stresses at the inner boundary at the central section for the three types of beams.

For the Arch beam for section ratios below 5

$$K = 0.834 + 1.504 \frac{h}{R_o + R_i}$$

and, for section ratios above 5 and below 10

$$K = 0.899 + 1.181 \frac{h}{R_o + R_i}$$

For Crescent I beams for section ratios below 2.00

$$K = 0.570 + 1.536 \frac{h}{R_o + R_i}$$

and for section ratios above 2.00 and below 10

$$K = 0.959 + 0.769 \frac{h}{R_o + R_i}$$

For Crescent II beams for section ratios below 10

$$K = 0.897 + 1.098 \frac{h}{R_o + R_i}$$

The location of the neutral surface was determined from fringe pattern photographs, and this information was expressed graphically. The distance from the centroid to the neutral surface increases as the section ratio decreases.

Stresses in non-central sections were determined. These stresses were smaller than the stress at the central section for the Arch beams. For the Crescent beams they were larger than the stress at the central section.

## CHAPTER I

### INTRODUCTION

This investigation was made to determine the stresses in eccentrically curved beams of low section ratio. These beams have circular-arc boundaries with different centers. The cross section is rectangular, and the depth of the cross section varies along the span of the beam. A photoelastic determination was made of stresses at the central sections and at non-central sections up to  $30^\circ$  away from the central section. Stress factors were determined, and these are expressed in empirical formulae for the range studied.

The principal difference between straight beams and curved beams is the mode of variation of unit-strain with the distance from the neutral surface. In the case of straight beams this variation is linear, but for curved beams it is non-linear. Concentrically curved beams are analyzed by the Winkler-Bach theory (1)\* which takes into account this non-linear variation. The need for information on eccentrically curved beams was first expressed by A. Becker (2) in 1946. Since that time J. P. Vidosic investigated this type of beam with section ratios varying from 6.5 to 100, and data and equations covering this range are now available (3), (4).

The purpose of this investigation is to expand the information into the region of lower section ratios as far as practical. The beams studied

---

\*Numbers in parenthesis identify references listed in Bibliography.

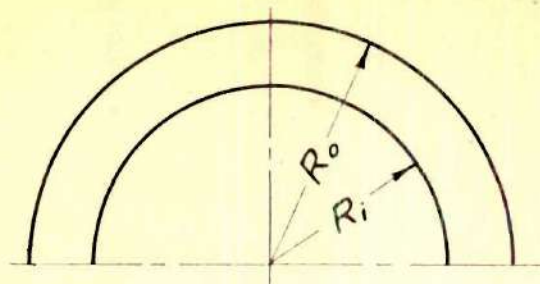
here are rectangular in cross section, are loaded in pure bending, and are symmetrical about the load plane. The centers of curvature of the outer and inner arcs lie on a straight line parallel to the lines of action of the applied loads. This straight line is the center line of the beam and lies in the central section.

Stress factors were obtained as the ratio of observed stresses to computed stresses in corresponding straight beams. The stress factors are compared by means of the parameter: the ratio of the sum of the radii of the arcs to the depth of the central section. This parameter is the section ratio.

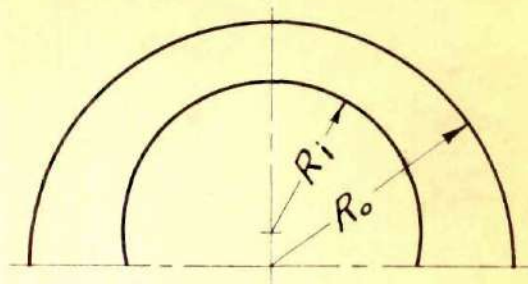
There are three types of eccentrically curved beams depending on the geometrical shapes. The "Arch" is the type in which the depth of the section increases with the distance from the central section. The "Crescent" is the type which has a corresponding decrease in depth of section. There are two divisions of the Crescent type. Crescent I has an outer radius larger than the inner radius, while Crescent II has an outer radius smaller than the inner radius. See Fig. 1.

All three types, the Arch, Crescent I, and Crescent II have been here investigated photoelastically in the region of the lower section ratios. The specific objectives have been:

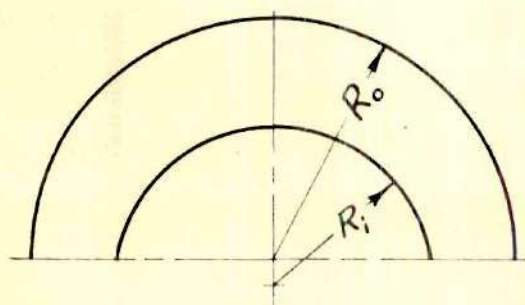
1. the determination of critical stresses (at central section) in beams of section ratio below 10 subjected to pure bending,
2. investigation of stresses in non-central sections, and
3. the establishment of rational stress equations for the range studied.



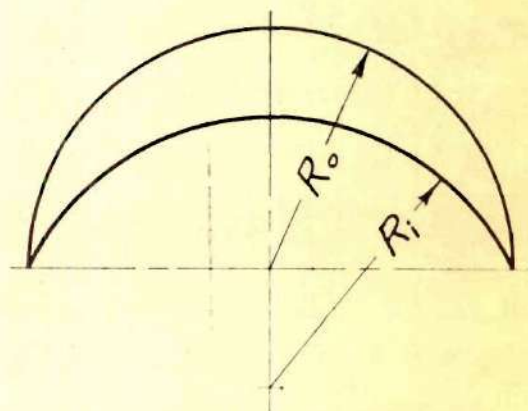
Concentric



Arch



Crescent I



Crescent II

Fig. 1. Types Of Curved Beams.

## CHAPTER II

### INSTRUMENTATION AND EQUIPMENT

Material.--All models tested in this investigation were cut from Columbia Resin CR-39.

Equipment.--The equipment required for performing the necessary laboratory research connected with this study may be divided into three classes:

1. equipment for cutting the models, 2. the polariscope, and 3. photographic equipment.

Cutting.--For the initial rough cut a jig saw running at its lowest speed was used. For precision cutting of the arcs and straight parallel lines a Gorton router was used. Three-directional feed is provided on this machine, and close tolerances may be maintained. The spindle rotates about a vertical axis, and the work is fed horizontally. Both 1/4 and 1/2 inch diameter cutters were used at a speed of 1370 revolutions per minute. The depth of cut varied between 0.005 and 0.01 inch. This cutting technique produced models without tooling stresses or wavy edges.

Two different jigs were used with the router, one for the circular arcs and the other for the straight-beam extensions. Each jig was a flat piece of steel plate, 5/16 inch thick, and each was provided with a number of drilled or tapped holes. Spacers 1/8 inch thick were placed between the model and the plate so that a full-depth cut might be possible. The model was held to the plate by steel straps or bars screwed to the plate.

For straight-line cuts the jig was bolted to the bed of the router, and the work was fed into the cutter in a longitudinal direction, while the depth of cut was regulated by feeding transversely. The jig used to cut the circular arcs was provided with four  $1/4$  inch diameter pivot holes drilled on the center line of the plate. A piece of  $1/4$  inch drill rod fixed vertically in the bed of the router served as the pivot. By rotating the jig about the pivot, exact circular arcs were cut on the model. See Fig. 2.

The Polariscopes.--A  $4-1/2$  inch polaroid-disk polariscope was used for the determination of the stresses needed in this investigation. The standard or "crossed circular" arrangement of elements was used because it gives clear, distinct fringe patterns (5). Fringe order values were converted to stress values by the application of the stress-optic law (6). Fractional fringe values were obtained by the Tardy method of rotation of the elements (7). Two light sources were available. White light was used for the general inspection of the model and for the study of isoclinics. A mercury vapor light filtered to monochromatic green (5,461 angstrom units) was used to produce sharper images for accurate fringe counts and for photographing.

The loading frame was located at the center of the polariscope. This frame consisted of a system of pin-connected linkages which loaded the model in pure bending. See Fig. 3. A spring-type scale was used to measure the applied load. The polarized image of the plastic model was projected upon a white screen for fringe order determination, or was focused upon a photographic negative for recording.

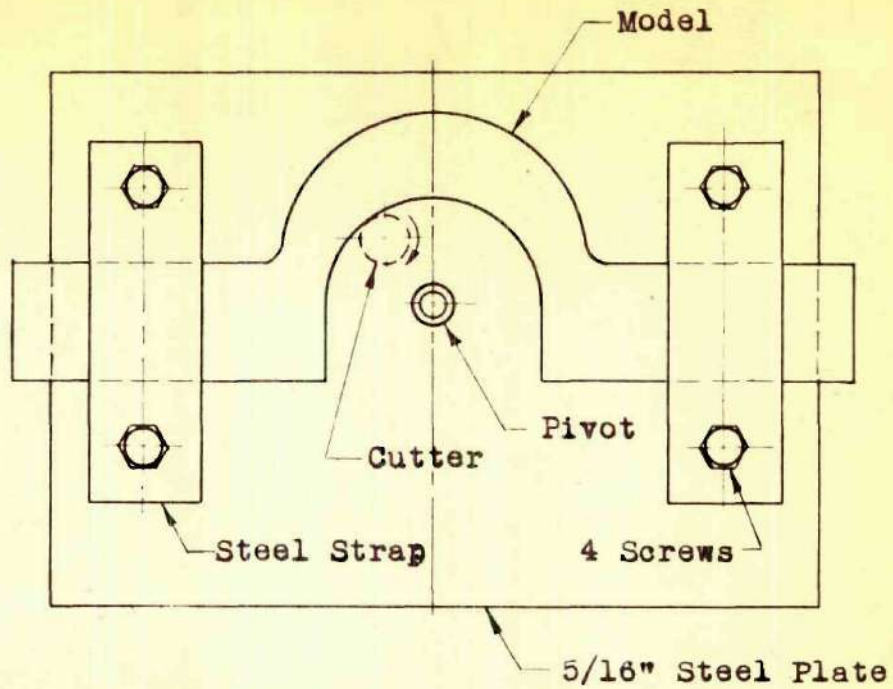


Fig. 2. Jig For Cutting Arcs.  
Model Shown in Place.

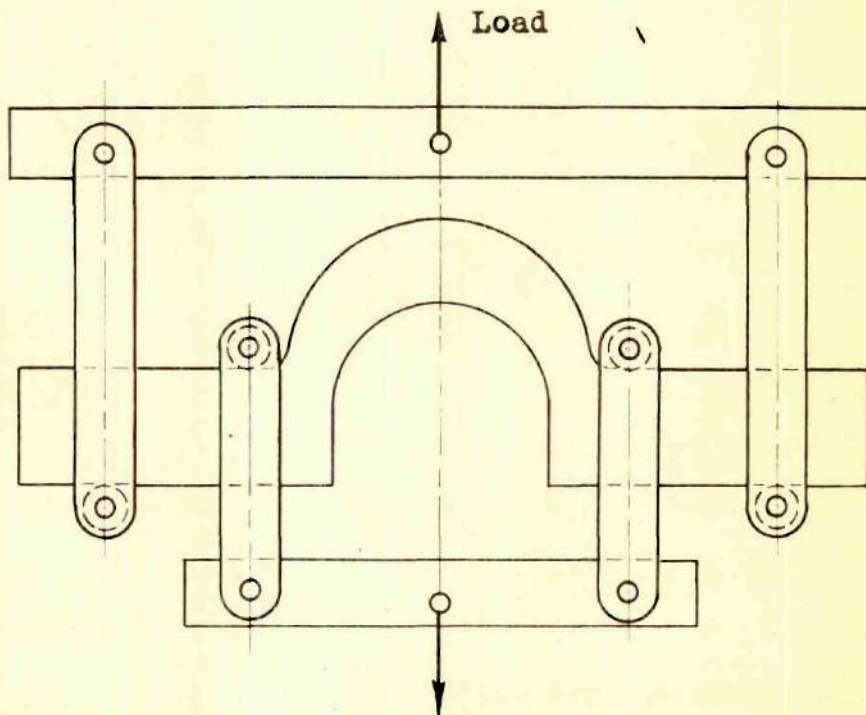


Fig. 3. Loading Frame With Model.

Photographic Equipment.---The Camera used with the polariscope had no lens since the lens system of the polariscope provided an image which could be focused directly onto the negative. Other photographic equipment consisted of the usual apparatus for developing, printing, and enlarging.

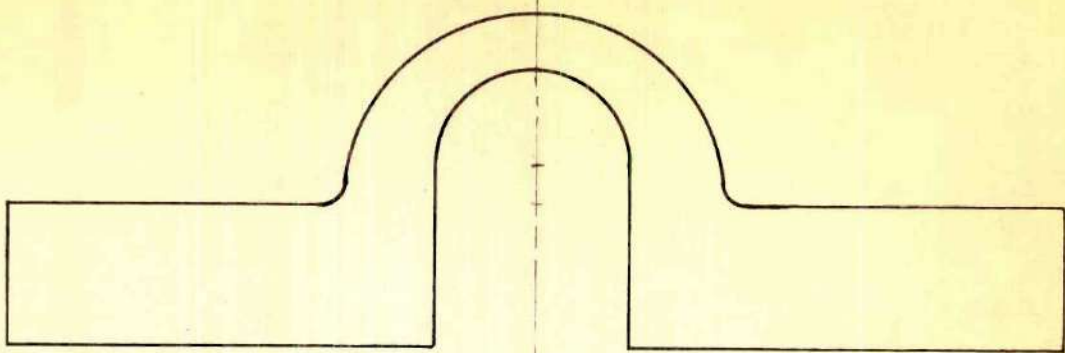
## CHAPTER III

### PROCEDURE

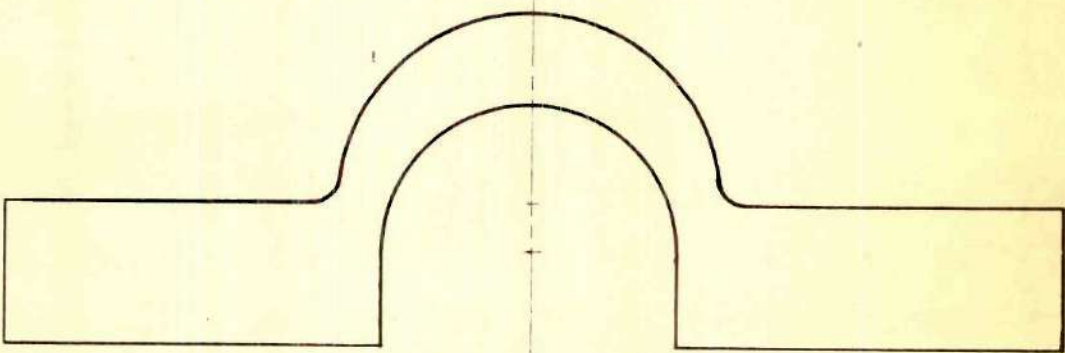
The size of the model was limited by the field of the polariscope. It was desired to study the stresses in the model up to a section removed from the central section by an angle of  $30^\circ$ . Lines were scribed at  $10^\circ$  intervals drawn from a point on the center line half way between the two arc centers. Therefore, in order to show all of the desired area it was necessary to cut the majority of the models with an outer radius in the neighborhood of one inch. For loading the model, extensions to the curved portion were provided to give a straight beam on each end. See Fig. 4. The loads were applied through needle-bearing rollers in contact with these straight beam extensions. There was some stress concentration at the junction of the straight and curved parts, but this was partially relieved by the use of fillets.

A concentric curved beam was prepared and used to observe the fringe pattern for this type of design. All fringes were observed to be concentric up to the close proximity of the fillets. They displayed no disturbances in the range to be studied --  $30^\circ$  either side of center. This led to the selection of the particular type model used in this investigation.

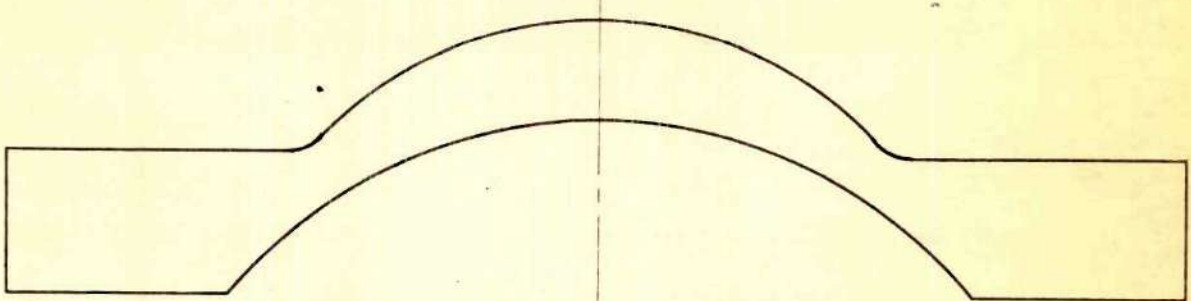
Other types of models were considered. One of these consisted of the curved beam only, with four holes drilled into the model for applying the loads. This type did not eliminate the problem of stress concentration,



Arch, No. 5.



Crescent I, No. 7.



Crescent II, No. 9.

Fig. 4. Full Size Drawings of Typical Models.

but increased it so as to reduce the unaffected field. A model of this type was cut and tested, but it fractured at the holes before enough load could be applied to obtain readings.

A layout of each model was scribed on a sheet of CR-39 before any cutting was done. After cutting with the jig saw, the model was given finish cuts by the router. The straight lines were cut first, then the curves. The scribed lines on the face of the model were used for aligning it on the jig. This alignment was accomplished by matching the scribed lines to a steel pointer held in the spindle chuck. Extreme care was needed here to produce a model which would give a symmetrical fringe pattern. The radius of the fillet at the junction of the straight and curved parts depended upon the size of the cutter used. This radius was either  $1/4$  or  $1/8$  inch. The height and depth of the central section were measured with a micrometer after the cutting was completed.

The examination of the model took place in the photoelastic dark-room where the temperature was held at  $68^{\circ}$  F. After the model was placed in the loading frame and initially loaded, a period of 30 minutes was allowed to elapse before any readings were made. A high initial creep is characteristic of CR-39, and the time allowance permits most of this creep to occur before any readings are made. Also, it allows the different models to be compared on the same basis. Fringe counts were made along the outer and inner boundaries at the central section and at sections removed from the central section by angles of 10, 20, and 30 degrees.

Calibration specimens were cut from the same pieces of material used for the curved beams. They were machined in the same manner on the

router, and were tested in the same way the curved beams were tested. These test specimens included tension models, compression models, and straight beam models subjected to pure bending. See Table 1 for calibration data.

The elastic range of CR-39 is from zero to about six or seven fringes. The loads applied to the models were limited so that the material was not stressed beyond its elastic range in the area studied. In only one case did the fringe order exceed six, and this value was 6.13.

## CHAPTER IV

## DISCUSSION OF RESULTS

All stress factors obtained apply to the central section and are based on the computed bending stress in a straight beam subjected to pure bending. The bending moment of the straight beam is the same as that carried by the curved beam being compared, and the cross-sectional dimensions are the same as those of the central section of the curved beam. Thus we have

$$K = \frac{\sigma_o}{S}$$

and

$$S = \frac{M}{Z} = \frac{6M}{bh^2}$$

Where  $K$  is the stress factor,  $\sigma_o$  is the observed stress at the central section, and  $S$  is the straight-beam stress.

The location of the neutral surface at the central section was established from photographed fringe patterns. This location was expressed as the ratio of the distance between the centroid of the section and the neutral surface,  $e$ , to the radius of curvature of the centroidal surface at the central section,  $R_c$ .  $R_c$  is taken as the average of the outer and inner radii.

Stresses at the inner boundary at non-central sections were compared to stresses at the inner boundary at the central section by the ratio  $\frac{\sigma_\theta}{\sigma_o}$ , where  $\sigma_\theta$  is the stress at the non-central section.

Empirical relations were established to express the variation of stress factors with section ratios for the range studied. This was done for stresses at the inner boundary of the central section only. No relations were found for the stress factors at the outer boundary since these values are less than one and are not critical in design. Relations involving the stress variations along the inner boundary of the beam were also established.

Arch Beams.--In this type of beam the depth of the section increases with the distance from the central section, and there is a corresponding decrease in stress. Therefore, designs based on the central section will be safe in pure bending.

Stresses were found experimentally and the stress factor K was computed. The values of K for both the inner and outer boundaries at the central section were plotted against the section ratio in Fig. 5. The curve for the stress factors at the inner boundary was drawn by using the empirical equations given below. These data for Arch beams are given in Table 2 in the Appendix.

To arrive at the proper form of an empirical equation various types of graphs were tried. It was found that the plot of K against the reciprocal of the section ratio gave practically a straight line, Fig. 13. Plots on "log" and "semi-log" graph paper produced definite curves. Therefore, the equation form

$$K = A + B \frac{h}{R_o + R_i}$$

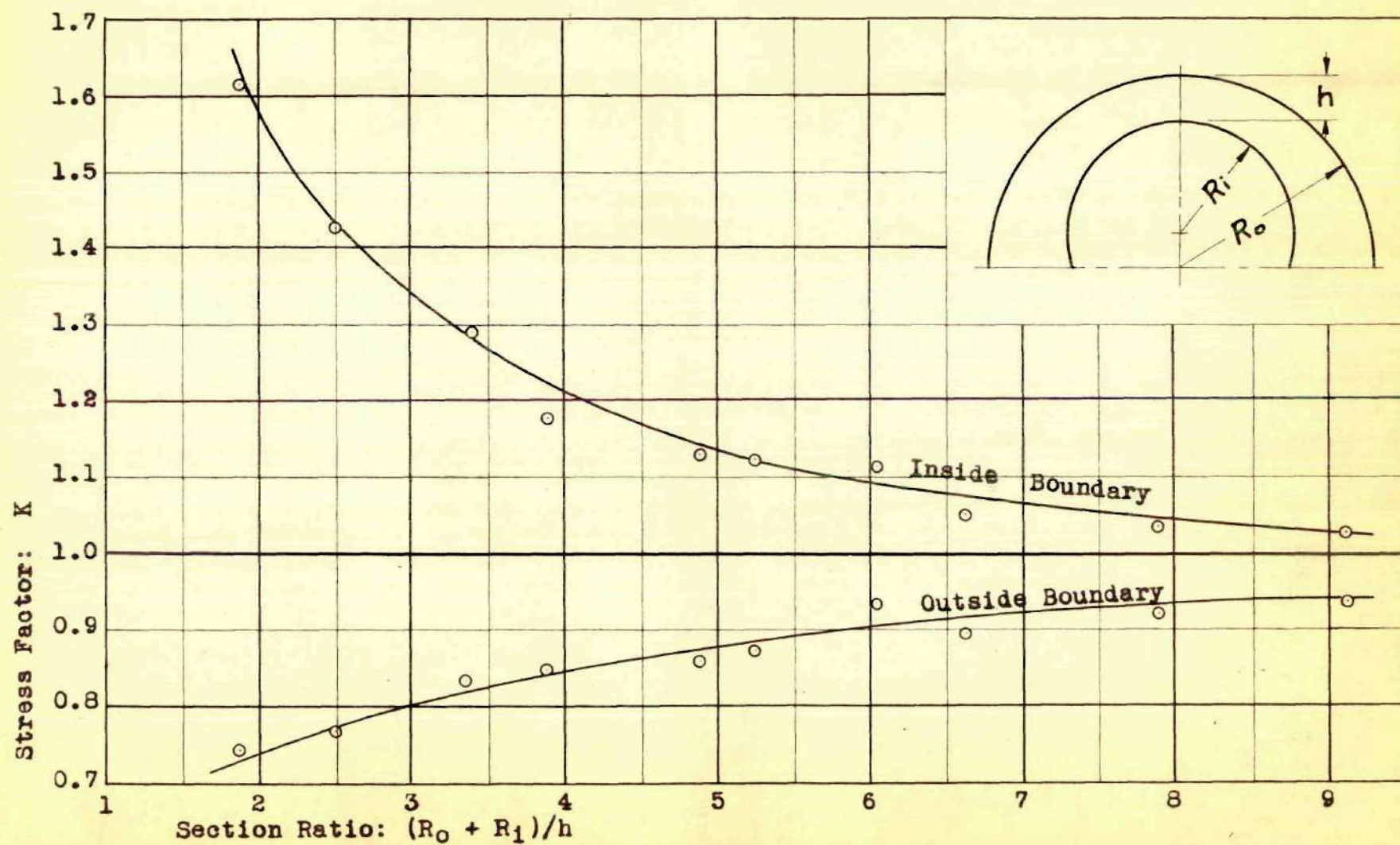
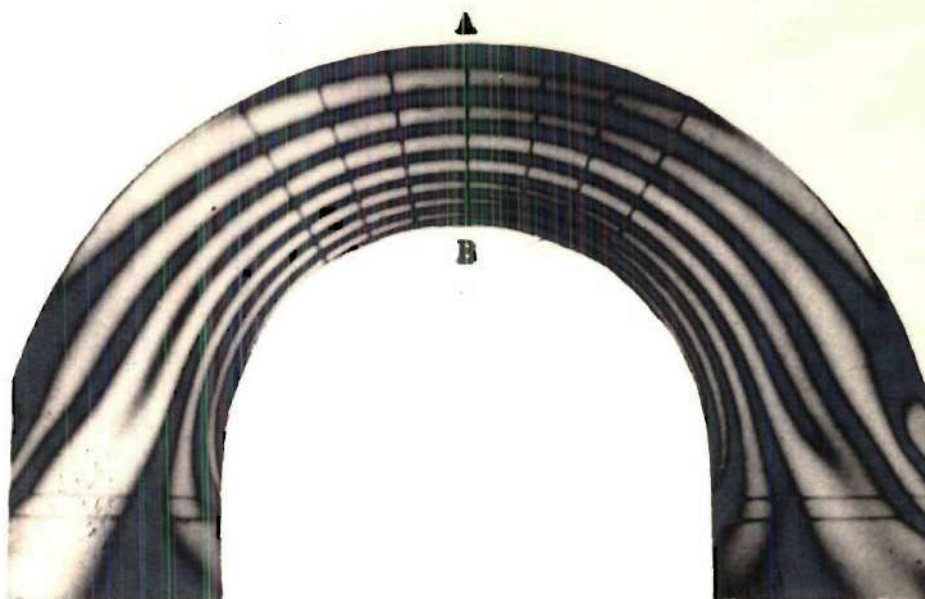
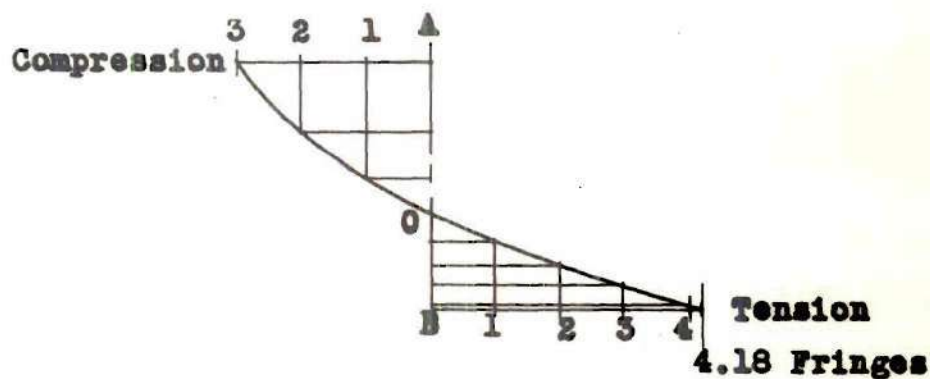


Fig. 5. Stress Factors For Arch Beams.



Photograph of Arch Beam No. 4.  
Made in Polariscope.



Stress Distribution at Central  
Section for Arch Beam No. 4.

Fig. 6. Photograph and Stress Distribution  
Curve for an Arch Beam.

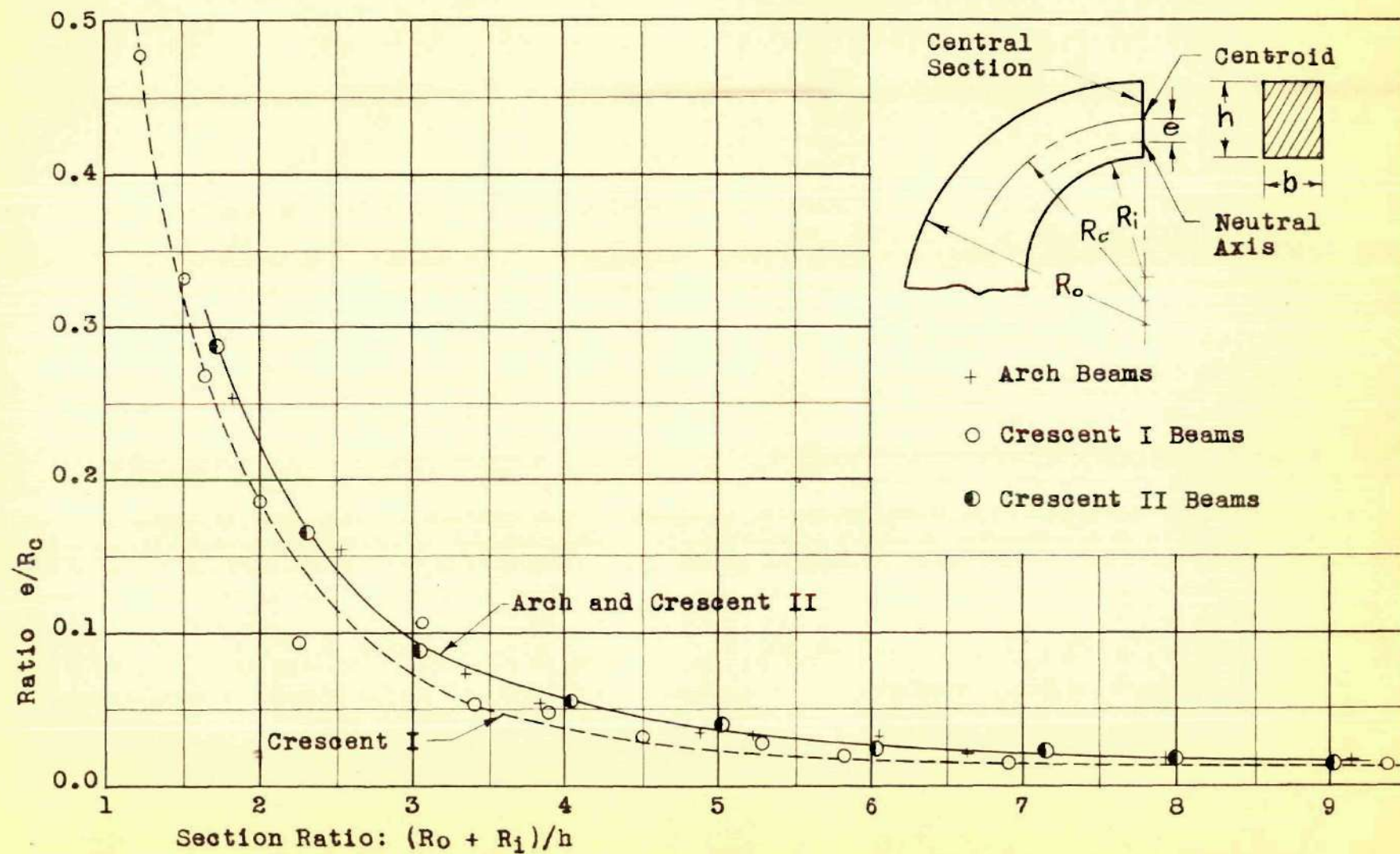


Fig. 7. Location Of Neutral Axis.

was used. The method of least squares was used to evaluate the constants A and B. Although this curve fit the points reasonably well, it crossed the line  $K = 1$  within the graph. This did not agree with the expected behavior of arch beams, as  $K$  should probably not be less than 1.00 for the inner boundary (8). Another equation was derived for the region above a section ratio of five, based on the observed values in this region. For the Arch beam the following equations were established: for section ratios below 5

$$K = 0.834 + 1.504 \frac{h}{R_o + R_i}$$

and, for section ratios above 5 and below 10

$$K = 0.899 + 1.181 \frac{h}{R_o + R_i} .$$

The location of the neutral surface is shown graphically in Fig. 7 for all three types of curved beams. Here the ratio  $e/R_o$  is plotted against the section ratio  $\frac{R_o + R_i}{h}$ . It is noted that the values for the Arch beam and the Crescent II beam are very close together, while those for the Crescent I beam are somewhat lower. The experimental data for this item are given in Table 5 in the Appendix.

Stresses in non-central sections were found to be less than those in the central section. The ratio of these stresses  $\sigma_\theta / \sigma_o$  was less than 1.00 for all Arch beams at all angles, and in each case the ratio decreased as the angle increased. See Table 6. However, there was actually very little decrease in most cases, and the results were scattered with no

definite pattern. Since the stresses in the non-central sections for the Arch beams are not of much practical importance, no empirical relation is suggested here.

Crescent I Beams.--In this type of beam the depth of the section decreases with the distance from the central section and the inner radius is smaller than the outer radius. As a result the stresses in the non-central sections are larger than those in the central section when the beam is loaded in pure bending.

Stress factors for the inner and outer boundaries at the central section for Crescent I beams are plotted against section ratios in Fig. 8. The curve for the stress factors at the inner boundary was drawn by using the empirical equations given below.

Tests were made to determine the proper form to be used for the empirical equations. The stress factor plotted against the reciprocal of the section ratio gave two distinct straight lines intersecting at a section ratio value of 2.00. Therefore, two separate equations were established. For section ratios from 1.25 to 2.00 the equation is

$$K = 0.570 + 1.536 \frac{h}{R_o + R_i}$$

and for section ratios above 2 and below 10

$$K = 0.959 + 0.769 \frac{h}{R_o + R_i}$$

The location of the neutral surface is shown graphically in Fig. 7 and the corresponding data given in Table 5.

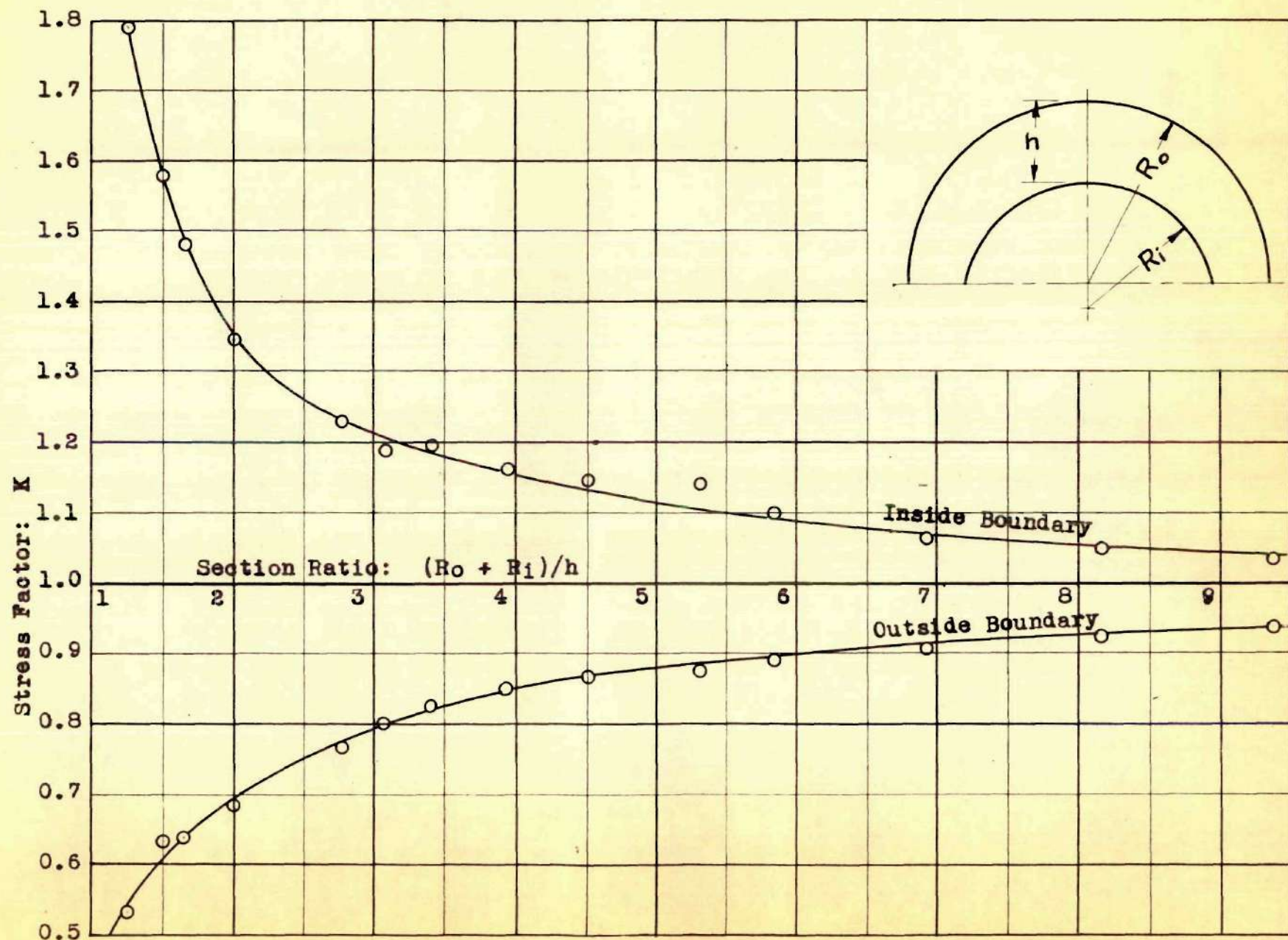
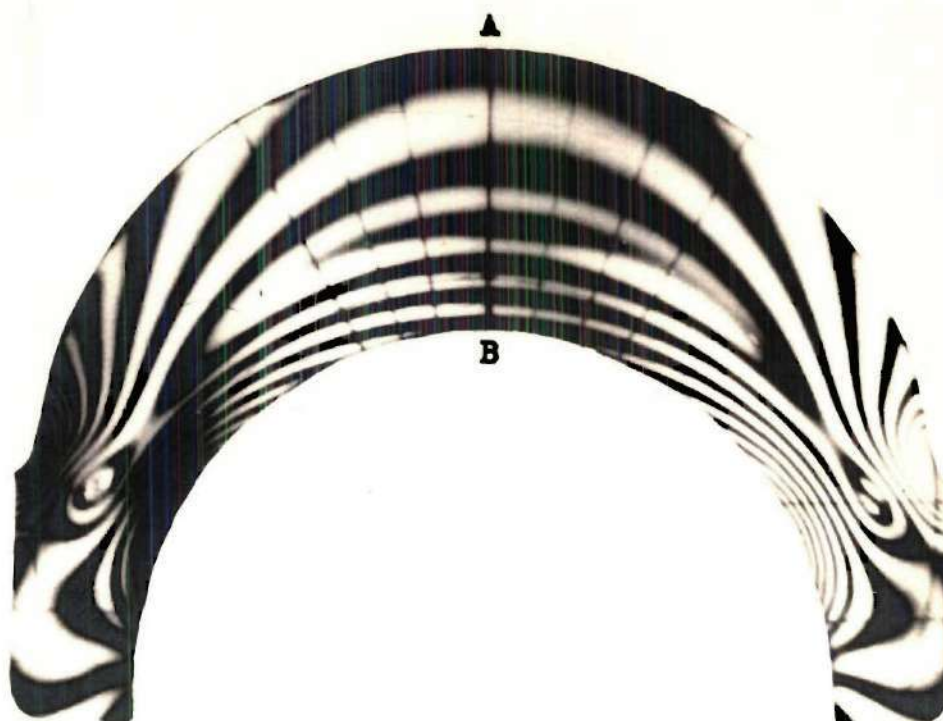
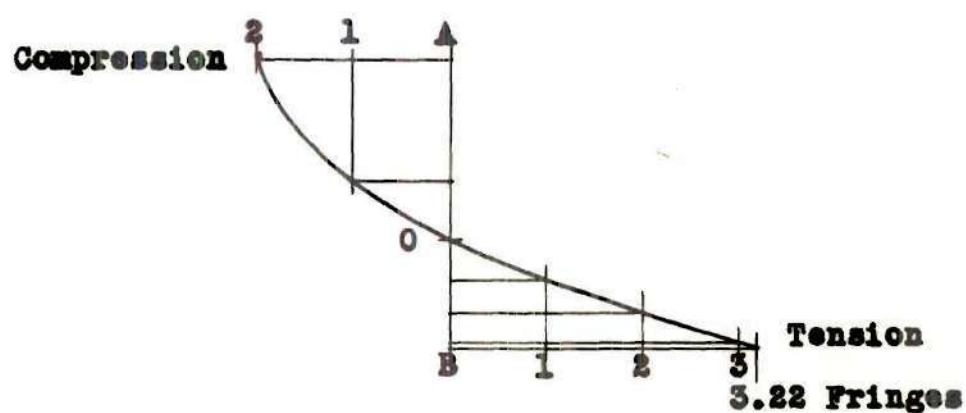


Fig. 8. Stress Factors For Crescent I Beams.



Photograph of Crescent I Beam No.  
5 Made in Polariscope.



Stress Distribution at Central Section  
for Crescent I Beam No. 5.

Fig. 9. Photograph And Stress Distribution  
Curve For A Crescent I Beam.

Stresses in non-central sections were referred to the central-section stress for the inner boundary by the ratio  $\frac{\sigma_{\theta}}{\sigma_0}$ . These ratios are given in Table 7. It was noted that these ratios increased as the angle increased, but there was no definite pattern of variation from model to model for any one angle. This is probably due to the differences in stress concentrations at the junction of the curved beam and the straight-beam extensions. It was found that the relation suggested by Vidosic (9) would serve adequately to express the stress ratio in terms of the angle. This equation is

$$\frac{\sigma_{\theta}}{\sigma_0} = \frac{1}{\cos^2 \theta}.$$

Values obtained from this equation are on the side of safety with the exception of the beam with a section ratio of 1.25, the lowest section ratio of the Crescent I series.

Crescent II Beams.---This type differs from the Crescent I type in that the inner radius is larger than the outer radius. The stresses in the non-central sections are greater than those in the central section.

Stress factors for the inner boundary at the central section for Crescent II beams are plotted against section ratios in Fig. 10. The curve for the stress factors at the inner boundary was drawn by using the empirical equation given below.

Tests to determine the proper equation form to be used here indicated that the reciprocal type could again be used, and that one equation would be sufficient. This equation is

$$K = 0.897 + 1.098 \frac{h}{R_0 + R_i}$$

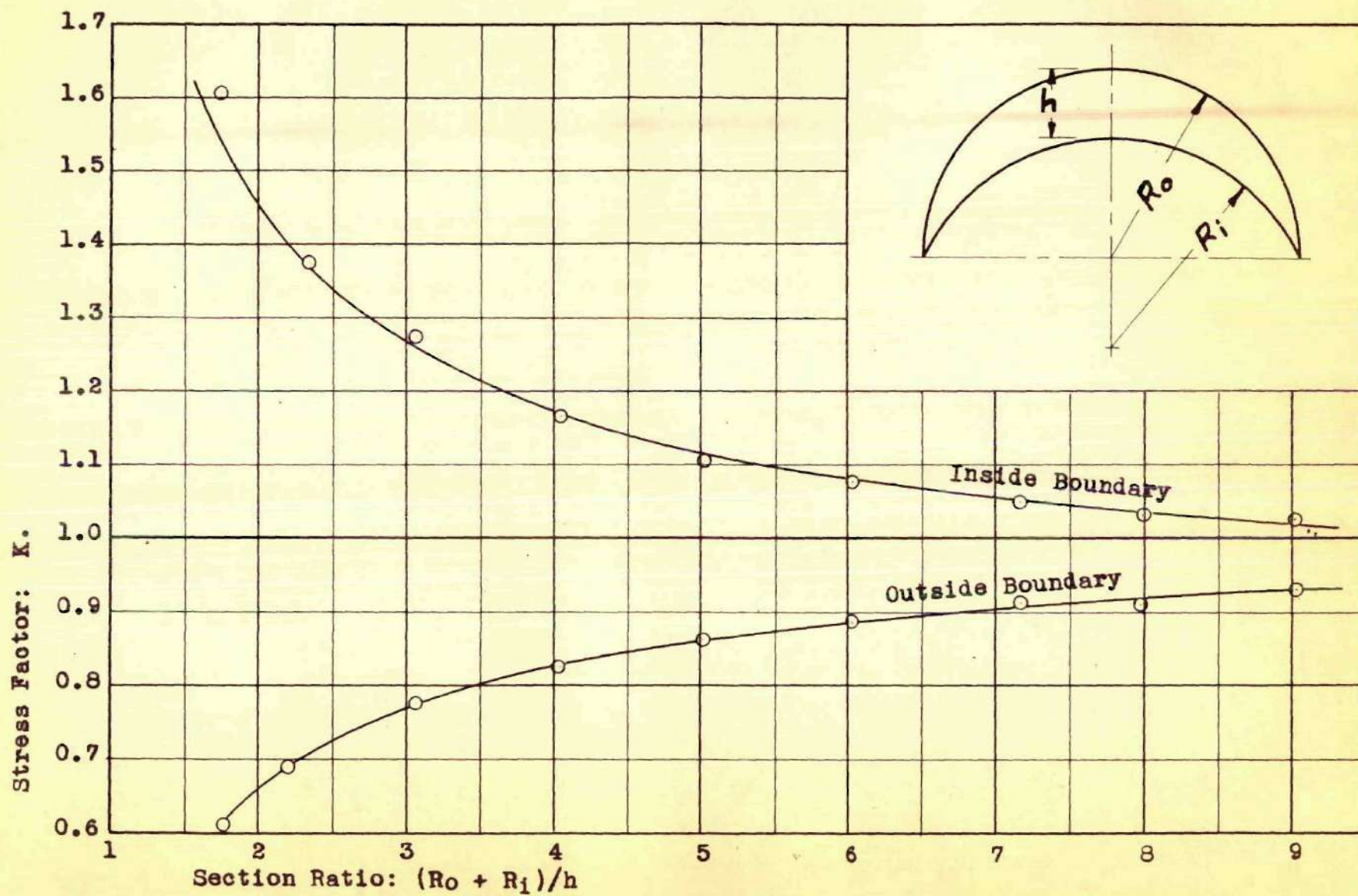
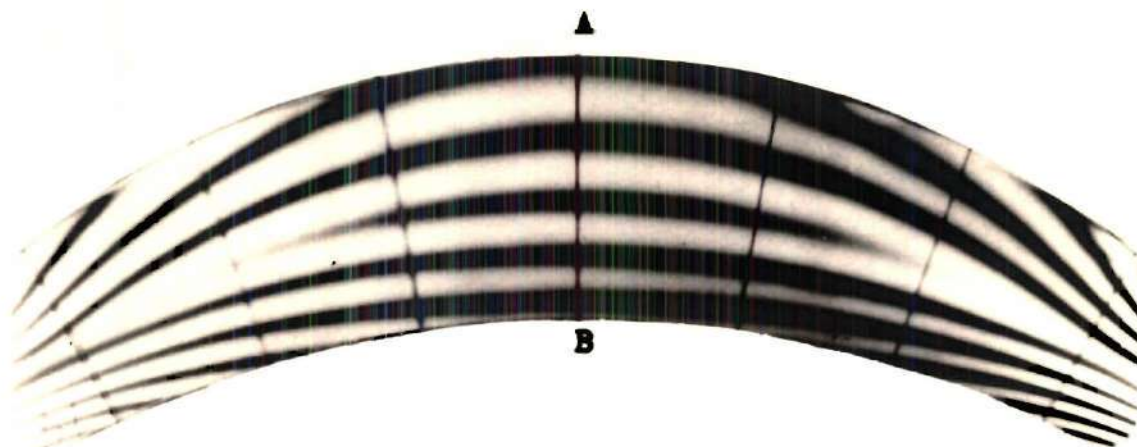
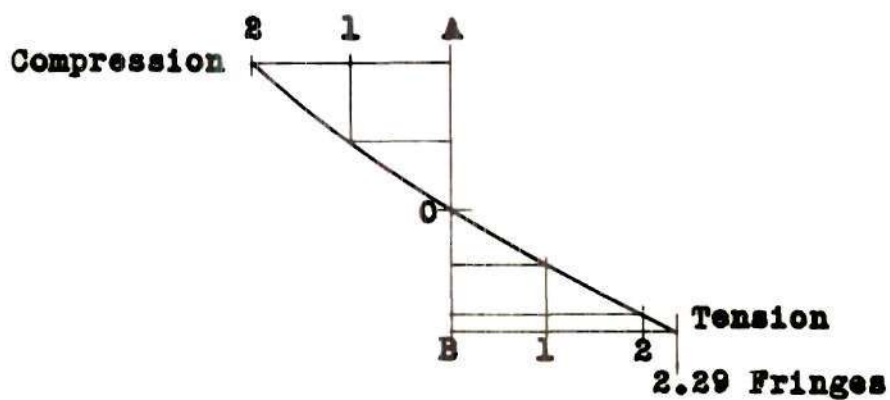


Fig. 10. Stress Factors for Crescent II Beams.



Photograph of Crescent II Beam  
No. 7 Made in Polariscope.



Stress Distribution at Central Section  
For Crescent II Beam No. 7.

Fig. 11. Photograph And Stress Distribution  
Curve for A Crescent II Beam.

The location of the neutral surface is shown graphically in Fig. 2, and the corresponding data is given in Table 5.

Stresses in the non-central sections were treated in the same manner as for the Crescent I beams. However, the ratios of stresses in the non-central sections to the stresses in the central sections were found to be considerably larger. See Table 8. The stress ratios increased as the angle from the central section increased, but there was no definite pattern of variation of stress ratios with section ratios. The following equation was derived to give the stress ratio in terms of the angle from the central section:

$$\frac{\sigma_{\theta}}{\sigma_0} = \frac{4.5}{\cos^2 \theta} - 3.5.$$

This equation gives stress ratios slightly larger than the largest ratio found, and it gives reasonable values for the remainder.

## CHAPTER V

### CONCLUSIONS

This investigation was made to determine the behavior of stresses in the three types of eccentrically curved beams. The photoelastic method was employed. The section ratios of the beams studied were below 10.

All models were rectangular in cross section and loaded in pure bending with the inner boundary in tension. Therefore, application of these results to other types of loading and section shapes must be made with due regard to factors that were not considered here.

The models were divided into three classes which depend upon the geometrical configuration. For the Arch beam the depth of the section was smallest at the central section. The Crescent types have their largest section depth at the central section. For the Crescent I beams the outer radius is larger than the inner radius, and for the Crescent II beams the inner radius is the larger.

For the Arch beams the greatest stress occurs at the inner boundary of the central section.

The larger stresses in the Crescent types are located along the inner boundary, and they increase with the distance from the central section.

Stress factors for the inner boundary at the central section for all three types of beams are greater than 1.00 for section ratios below 10, that is, the stress for this location is larger than the stress in

the corresponding straight beam. For all three types, the stress at the outer boundary at the central section is smaller than the stress in the corresponding straight beam.

For all types, the stress factors for the inner boundary at the central section increase as the section ratios decrease.

All stresses considered in this study are located along the boundary, and, therefore, are tangent to the boundary arc. Since the models were loaded in pure bending, no shear stresses are considered.

## CHAPTER VI

### RECOMMENDATIONS

Possible sources of error involved in the photoelastic method make it desirable that final conclusions be made only after a very large number of tests have been made. Since the number of tests made here were necessarily limited, it is in order that additional data be accumulated by others. Also, to make the information more complete, other means of experimental stress analysis should be employed.

Other problems in conjunction with this one that should prove of interest to one working with photoelasticity are: the investigation of stresses within the body of the curved beam, loading to produce tension in the outer boundary, loading other than pure bending, the use of other types of cross sections, further investigation of stresses in non-central sections with different means of applying loads, and further investigation of beams of extremely low section ratio (below 2).

In the case of the last item mentioned above, beams of extremely low section ratio of the Crescent I type were found to have an unusual distribution of stress along the depth of the beam at the central section. See Fig. 12. As one moves outward along the central section beyond the neutral surface, the stress increases and then decreases. Ordinarily the stress continues to increase until the outer boundary is reached. It might be said that the "beam" is no longer a beam, but is an "eccentric shape." The investigation and explanation of this effect should prove of interest.

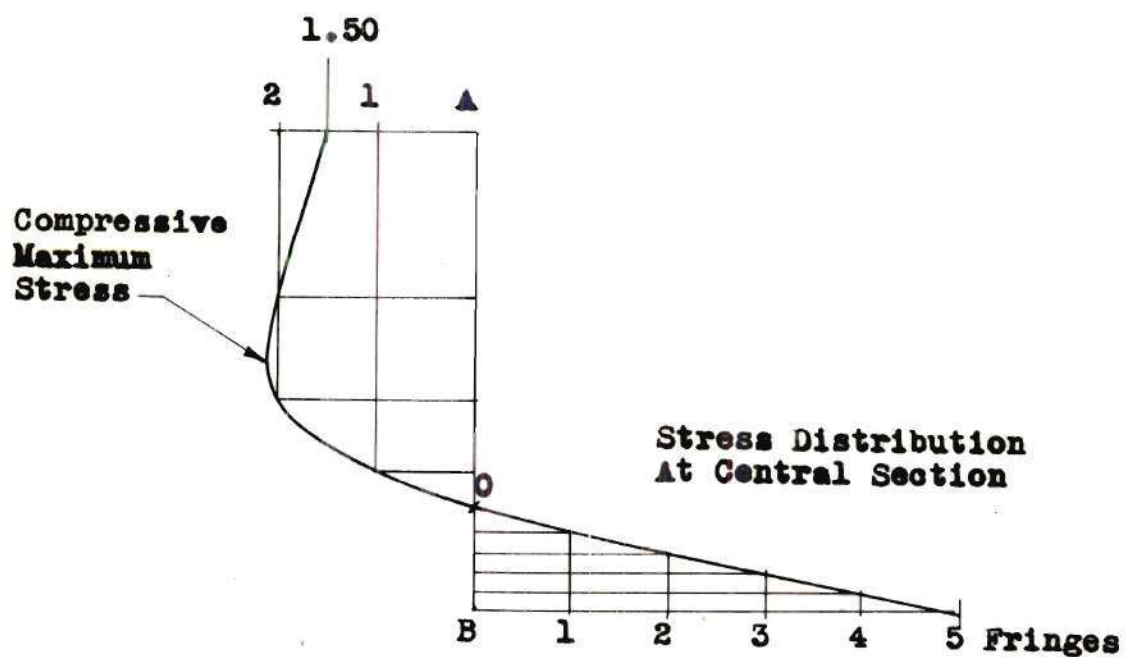
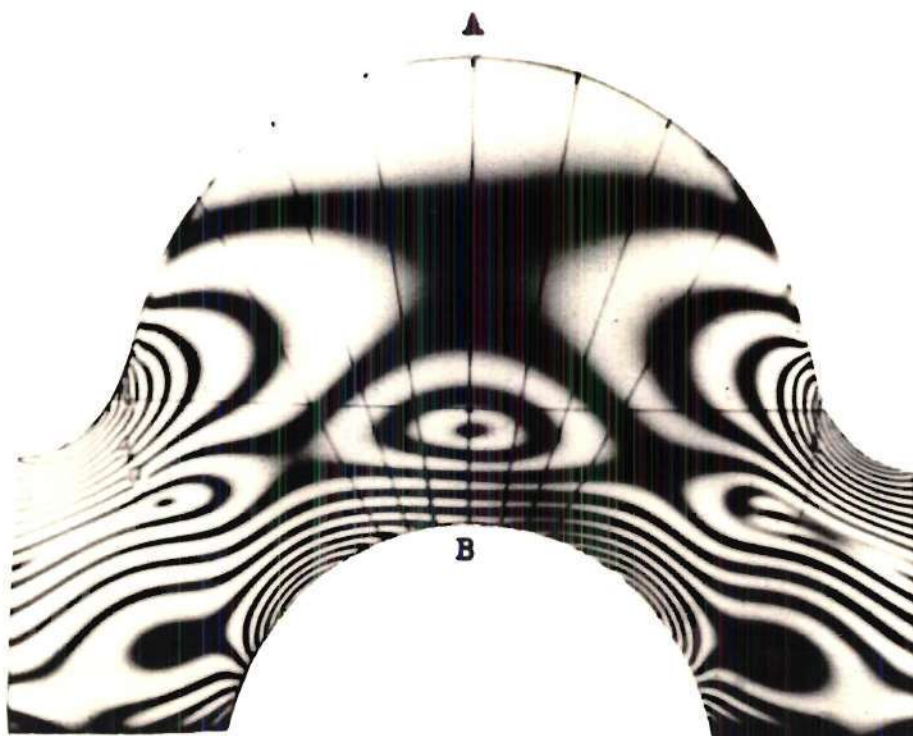


Fig. 12. Photograph and Stress Distribution Curve For Crescent I No. 1.

## APPENDIX

Table 1. Calibration Data - CR 39

Test No.	Group No.	Type Test	Dimensions b in. h in.		Load (lb.) or Moment (lb.in.)	Fringe Order, n	Material Fringe Value = f lb./in.Fr.
1	1	Comp.	0.215	0.928	272 lb.	4.00	36.8
2	2	Comp.	0.235	0.750	237 lb.	4.00	39.5
3	2	Bending	0.227	0.749	30.9 lb.in.	4.00	41.4
4	2	Tens.	0.228	0.501	77 lb.	2.00	38.4
5	3	Tens.	0.236	0.498	80 lb.	2.00	40.2
6	3	Tens.	0.245	0.510	80 $\frac{1}{2}$ lb.	2.00	39.4
7	3	Comp.	0.241	0.649	153 lb.	3.00	39.4
8	3	Comp.	0.245	0.510	125 lb.	3.00	40.8
9	3	Bending	0.244	0.624	22.7 in.lb.	4.00	41.3

Group No.	Average Material Fringe Value f	Model Numbers for Which f Applies
1	36.8	Crescent I: No. 6
2	39.8	Crescent I: Nos. 2, 3, 4, 5, 7, 8, 9, 10, 11, 12
3	40.2	Crescent I: Nos. 1, 13, 14, Crescent II: All Arch Beams: All

Table 2. Arch Beam Data

No.	Outer Radius	Inner Radius	Section Width	Section Depth	Bending Moment, M	Fringe Order	
	$R_o$ in.	$R_i$ in.				Outer Arc, n Fringes	Inner Arc, n Fringes
1	1	1/4	0.240	0.671	16.33	2.00	4.39
2	1	1/4	0.240	0.497	9.45	2.18	4.08
3	1	1/2	0.243	0.446	10.31	3.21	5.00
4	1	1/2	0.243	0.386	7.08	3.00	4.18
5	1	1/2	0.244	0.307	5.58	3.76	5.00
6	1	5/8	0.242	0.309	5.15	3.50	4.53
7	1	1/2	0.244	0.247	3.66	4.17	5.00
8	1	5/8	0.242	0.244	3.66	4.06	4.79
9	1	3/4	0.240	0.221	2.15	3.00	3.38
10	1	49/64	0.240	0.193	1.61	3.00	3.29

No.	Section Ratio $(R_o + R_i)/h$	Straight-Beam Stress $S = 6M/bh^2$ psi	Stresses at Central Section		Stress Factors	
			$\sigma_o$ psi	$\sigma_i$ psi	$K_o$	$K_i$
1	1.87	907	670	1470	0.739	1.620
2	2.51	957	731	1368	0.764	1.428
3	3.36	1281	1063	1655	0.830	1.291
4	3.89	1175	993	1383	0.845	1.179
5	4.89	1455	1238	1645	0.852	1.130
6	4.26	1336	1161	1502	0.870	1.125
7	6.08	1474	1373	1645	0.932	1.116
8	6.66	1518	1351	1590	0.890	1.049
9	7.92	1095	1005	1132	0.918	1.033
10	9.15	1071	1005	1103	0.937	1.028

Table 3. Crescent I Data

No.	Outer Radius $R_o$ in.	Inner Radius $R_i$ in.	Section Width $b$ in.	Section Depth $h$ in.	Bending Moment, $M$ in. lb.	Fringe Order	
						Outer Arc, $n$ Fringes	Inner Arc, $n$ Fringes
1	3/4	1/2	0.234	1.001	36.29	1.50	5.04
2	1	1/2	0.228	0.989	41.02	2.00	5.00
3	1	9/16	0.228	0.937	36.51	2.00	4.63
4	1	3/4	0.231	0.870	30.93	2.09	4.13
5	1	3/4	0.234	0.627	13.73	2.00	3.22
6	1	3/4	0.218	0.569	9.88	2.00	2.97
7	1	3/4	0.234	0.512	11.82	2.80	4.00
8	1	3/4	0.218	0.444	9.02	3.00	4.11
9	1	3/4	0.239	0.386	6.88	3.00	4.00
10	1	3/4	0.239	0.329	4.82	3.00	3.93
11	1	7/8	0.229	0.321	3.22	2.02	2.50
12	1	7/8	0.229	0.271	2.15	2.00	2.34
13	1	7/8	0.239	0.229	1.61	2.13	2.40
14	1	7/8	0.239	0.204	1.72	2.89	3.18

No.	Section Ratio $(R_o + R_i)/h$	Straight-Beam Stress $S = 6M/bh^2$ psi	Stresses at Central Section		Stress Factors	
			$\sigma_o$ psi	$\sigma_i$ psi	$K_o$	$K_i$
1	1.25	965	516	1731	0.535	1.795
2	1.52	1104	698	1745	0.631	1.580
3	1.67	1093	698	1618	0.638	1.479
4	2.01	1063	722	1425	0.679	1.341
5	2.79	893	682	1099	0.764	1.230
6	3.08	841	672	999	0.800	1.187
7	3.42	1156	955	1364	0.826	1.193
8	3.94	1260	1071	1468	0.850	1.165
9	4.53	1160	999	1332	0.862	1.149
10	5.32	1145	999	1308	0.872	1.141
11	5.85	792	705	872	0.890	1.102
12	6.93	767	696	815	0.907	1.063
13	8.18	770	715	806	0.928	1.048
14	9.38	1034	971	1069	0.939	1.031

Table 4. Crescent II

No.	Outer Radius	Inner Radius	Section Width	Section Depth	Bending Moment, M	Fringe Order	
	$R_o$ in.	$R_i$ in.				Outer Arc, n Fringes	Inner Arc, n Fringes
1	3/4	1	0.239	0.992	16.38	0.76	2.00
2	3/4	1	0.239	0.748	10.92	1.00	2.00
3	1	1-1/4	0.239	0.734	11.37	1.22	2.00
4	1	1-1/4	0.239	0.556	10.08	2.00	2.82
5	2	3	0.239	0.997	24.72	1.60	2.04
6	2	2-1/2	0.239	0.747	16.93	2.00	2.43
7	2	2-1/2	0.239	0.628	11.58	2.00	2.29
8	2	2-1/2	0.239	0.563	9.37	2.00	2.26
9	2	2-1/2	0.239	0.498	7.13	2.00	2.21

No.	Section Ratio $(R_o + R_i)/h$	Straight-Beam Stress $S = 6M/bh^2$ psi	Stresses at Central Section		Stress Factors	
			$\sigma_o$ psi	$\sigma_i$ psi	$K_o$	$K_i$
1	1.77	420	256	674	0.610	1.604
2	2.34	490	337	674	0.688	1.373
3	3.07	529	412	674	0.779	1.272
4	4.05	816	674	950	0.826	1.163
5	5.02	623	539	687	0.865	1.102
6	6.03	764	674	819	0.882	1.072
7	7.18	736	674	772	0.915	1.049
8	7.99	740	674	762	0.910	1.031
9	9.03	722	674	742	0.933	1.029

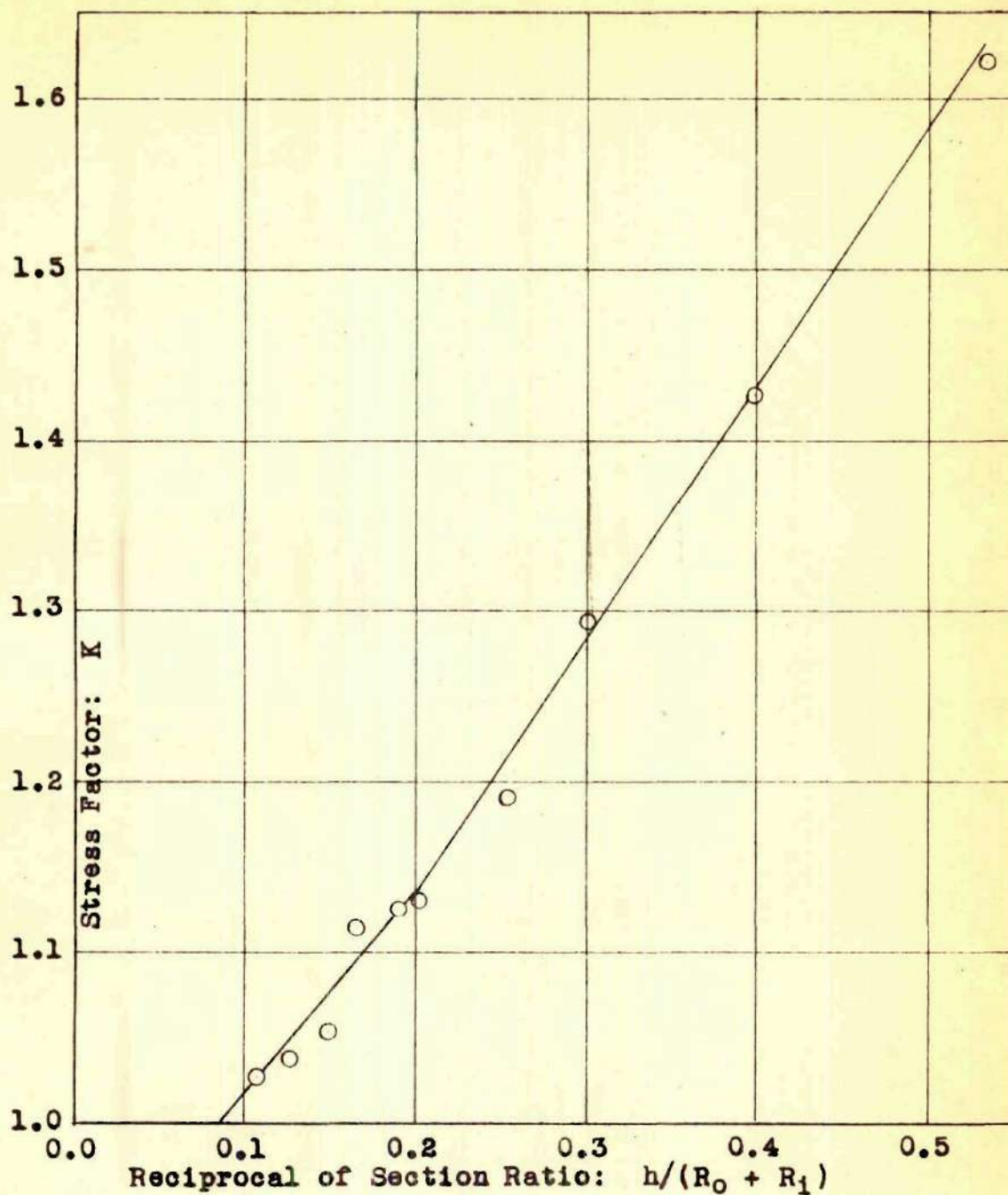


Fig. 13. Plot of Stress Factors and Reciprocals of Section Ratios for Arch Beams.

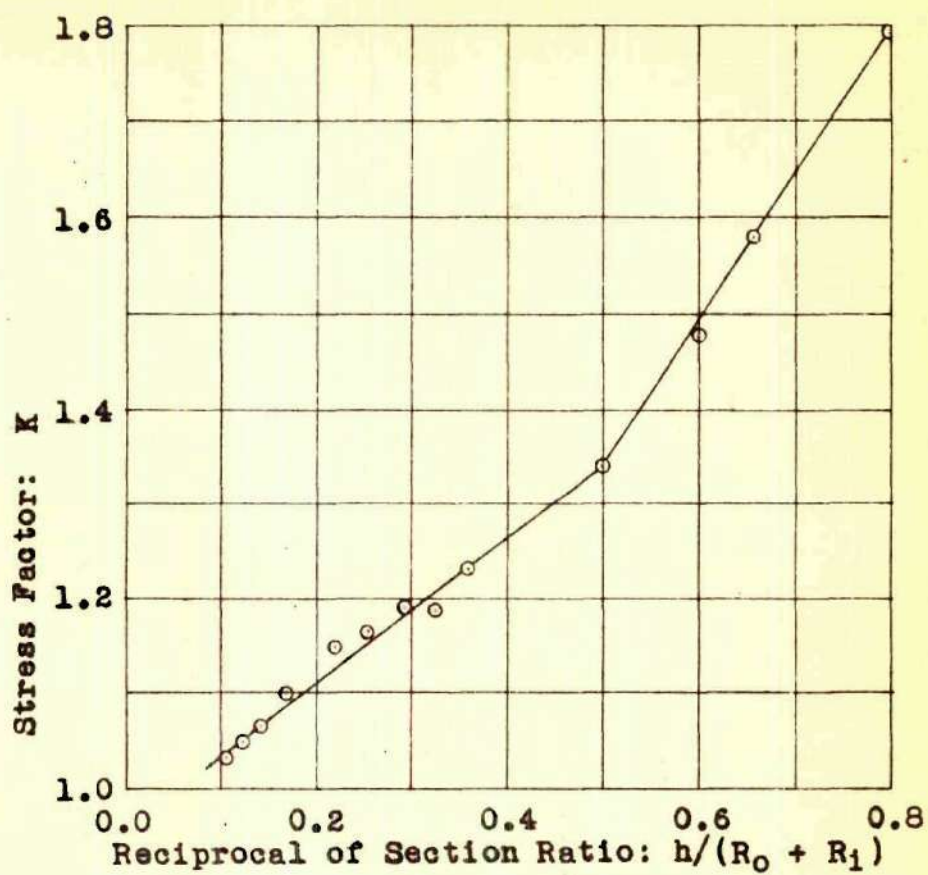


Fig. 14. Plot of Stress Factors and Reciprocals of Section Ratios for Crescent I Beams.

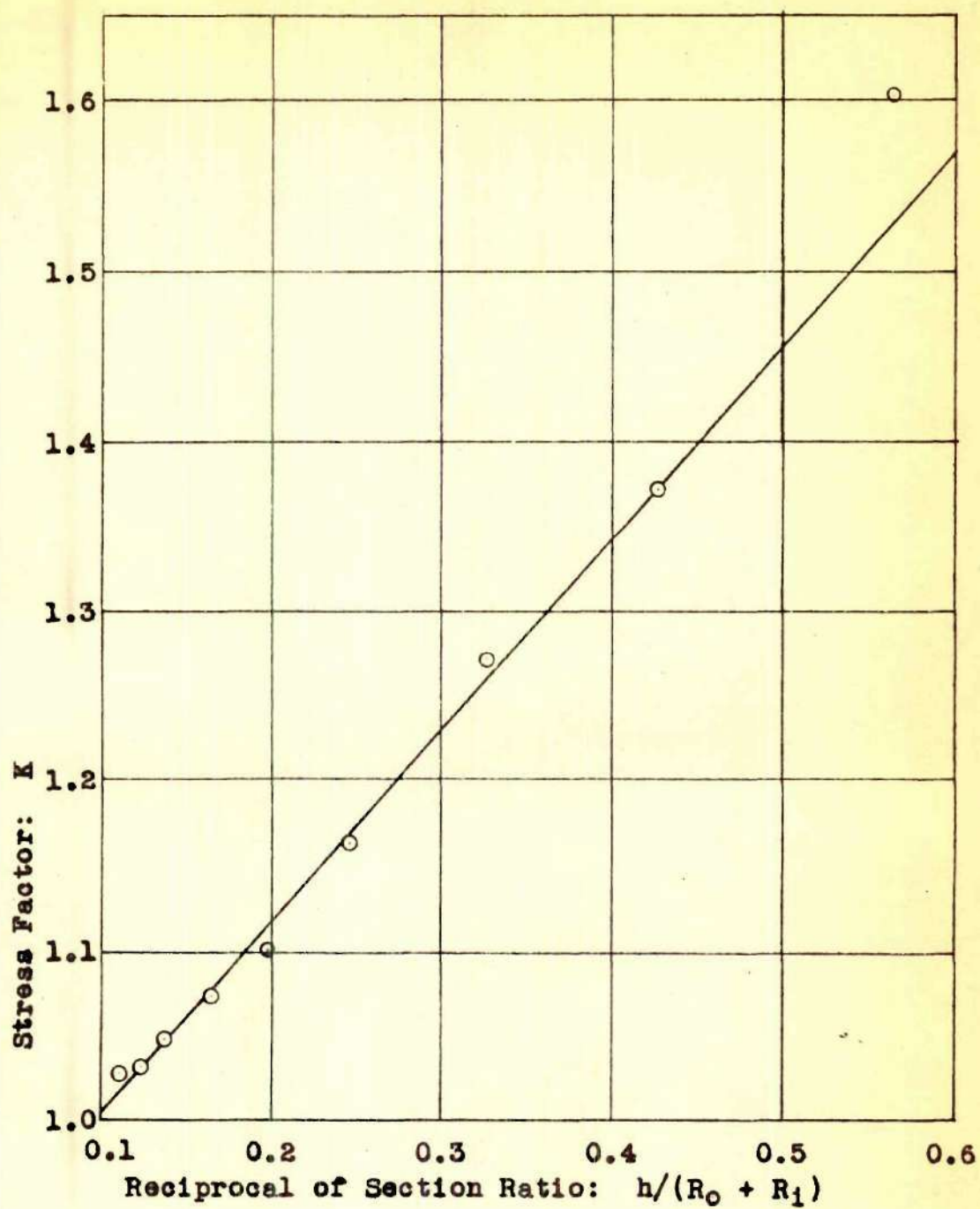


Fig. 15. Plot of Stress Factors and Reciprocals of Section Ratios for Crescent II Beams.

Table 5. Location of Neutral Surface at Central Section

ARCH BEAMS			CRESCENT I BEAMS		
No.	Section Ratio ( $R_o + R_i$ )/h	Offset Ratio e/ $R_c$	No.	Section Ratio ( $R_o + R_i$ )/h	Offset Ratio e/ $R_c$
1	1.87	0.2531	1	1.25	0.4770
2	2.51	0.1552	2	1.52	0.3349
3	3.36	0.0721	3	1.67	0.2676
4	3.89	0.0524	4	2.01	0.1840
5	4.89	0.0348	5	2.79	0.0896
6	5.26	0.0335	6	3.08	0.1092
7	6.08	0.0316	7	3.42	0.0532
8	6.66	0.0196	8	3.94	0.0538
9	7.92	0.0182	9	4.53	0.0327
10	9.15	0.0159	10	5.32	0.0297
			11	5.85	0.0195
			12	6.93	0.0130
			13	8.18	--
			14	9.38	0.0120

CRESCENT II BEAMS		
No.	Section Ratio ( $R_o + R_i$ )/h	Offset Ratio e/ $R_c$
1	1.77	0.2872
2	2.34	0.1633
3	3.07	0.0893
4	4.05	0.0563
5	5.02	0.0399
6	6.03	0.0243
7	7.18	0.0226
8	7.99	0.0137
9	9.03	0.0121

Table 6. Stresses in Non-Central Section for Arch Beams  
At Inside Boundary

No.	Stress in Fringes At Angle $\theta =$				Stress Ratio $\sigma_{\theta}/\sigma_0$ For		
	0°	10°	20°	30°	10°	20°	30°
1	4.39	--	--	4.35	--	--	0.992
2	4.08	4.04	4.00	3.83	0.989	0.980	0.939
3	5.00	--	--	4.87	--	--	0.975
4	4.18	4.12	4.05	4.00	0.987	0.970	0.958
5	5.00	4.90	4.78	4.46	0.980	0.956	0.892
6	4.53	4.42	4.34	4.31	0.978	0.957	0.951
7	5.00	4.91	4.44	3.93	0.985	0.888	0.786
8	4.79	4.75	4.59	4.30	0.992	0.938	0.898
9	3.38	3.33	3.23	3.17	0.985	0.956	0.938
10	3.29	3.25	3.18	3.06	0.988	0.967	0.931

Table 7. Stresses in Non-Central Sections at Inside Boundary  
For Crescent I Beams

No.	Stress in Fringes At Angle $\theta =$				Stress Ratio $\sigma_{\theta} / \sigma_0$ For		
	$0^\circ$	$10^\circ$	$20^\circ$	$30^\circ$	$10^\circ$	$20^\circ$	$30^\circ$
1	5.04	5.62	5.90	6.13	1.116	1.172	1.216
2	5.00	5.13	5.22	5.41	1.026	1.044	1.082
3	4.63	4.74	5.00	5.16	1.023	1.080	1.115
4	4.13	4.20	4.23	4.89	1.018	1.025	1.181
5	3.22	3.25	3.37	3.56	1.010	1.046	1.105
6	2.97	3.06	3.17	3.31	1.031	1.068	1.114
7	4.00	4.10	4.22	4.56	1.025	1.055	1.140
8	4.11	4.17	4.26	4.39	1.015	1.038	1.069
9	4.00	4.01	4.03	4.04	1.003	1.008	1.010
10	3.93	3.95	4.01	4.13	1.005	1.021	1.050
11	2.50	2.54	2.81	2.94	1.015	1.123	1.175
12	2.34	2.36	2.39	2.52	1.008	1.021	1.077
13	2.40	2.42	2.57	3.08	1.007	1.070	1.282
14	3.18	3.27	3.54	3.85	1.028	1.113	1.211
				$\frac{1}{\cos^2 \theta}$	1.031	1.132	1.333

Table 8. Stresses in Non-Central Sections at Inside Boundary  
For Crescent II Beams

No.	Stress in Fringes At Angle $\theta =$				Stress Ratio $\sigma_{\theta} / \sigma_0$ For		
	0°	10°	20°	30°	10°	20°	30°
1	2.00	2.08	2.39	3.02	1.040	1.195	1.510
2	2.00	2.16	2.92	4.49	1.080	1.460	2.245
3	2.00	2.18	2.74	4.00	1.090	1.370	2.000
4	2.82	3.00	3.45	4.11	1.065	1.223	1.456
5	2.04	2.16	2.91	4.17	1.059	1.426	2.045
6	2.43	2.47	3.09	4.40	1.018	1.273	1.812
7	2.29	2.45	3.08	4.21	1.071	1.345	1.837
8	2.26	2.51	3.25	5.11	1.110	1.440	2.308
9	2.21	2.51	3.20	5.36	1.135	1.450	2.460
$\frac{4.5}{\cos^2 \theta} - 3.5$					1.14	1.60	2.50

## NOMENCLATURE

$A, B$	=	empirical constants
$b$	=	width of cross section in inches
$e$	=	distance between centroid of section and neutral surface
$f$	=	material fringe value
$h$	=	depth of cross section in inches
$k$	=	stress factor
$k_i$	=	stress factor for inside boundary
$k_o$	=	stress factor for outside boundary
$M$	=	bending moment in pound - inches
$n$	=	fringe order
$R$	=	radius
$R_c$	=	radius of centroidal surface at central section
$R_i$	=	radius of inner boundary arc
$R_o$	=	radius of outer boundary arc
$S$	=	theoretical bending stress for a straight beam in lb/in <sup>2</sup>
$Z$	=	section modulus in in <sup>3</sup>
$\theta$	=	angle between plane of central section and plane of non-central section
$\sigma$	=	observed stress
$\sigma_o$	=	observed stress at central section
$\sigma_\theta$	=	observed stress at non-central section removed from central section by angle $\theta$

## BIBLIOGRAPHY

1. Seely, Fred B., Advanced Mechanics of Materials, New York: John Wiley and Sons, Inc., 1932, p. 110.
2. Becker, H., "Photoelastic Analysis of a Spar Bulkhead," Proceedings of the Society for Experimental Stress Analysis IV, 1946, p. 43.
3. Vidosic, J. P., Stress Relation Factors for Curved Beams Having Eccentric Boundaries, Unpublished Ph.D. Thesis, Purdue University, 1951.
4. Vidosic, J. P., "Bending Stresses in Eccentric Curved Beams," Product Engineering, 22, November 1951, pp. 180-183.
5. Frocht, M. M., Photoelasticity, Vol. 1, New York: John Wiley and Sons, Inc., 1941, p. 125.
6. Ibid., p. 136.
7. Jessop, H. T. and Harris, F. C., Photoelasticity, New York: Dover Publications, Inc., 1950, p. 72, p. 176.
8. Vidosic, J. P., Ph. D. Thesis, p. 22.
9. Ibid., p. 23.